

# Micro ring laser cavity design for biosensing

Lantian Chang<sup>1</sup>, Michiel de Goede<sup>1</sup>, Meindert Dijkstra<sup>1</sup> and Sonia M. García-Blanco<sup>1</sup>

<sup>1</sup> Optical Sciences Group, MESA+ Institute for Nanotechnology, University of Twente, P.O. Box 217, 7500 AE Enschede, The Netherlands

*We proposed a micro ring laser cavity design methodology for biosensing application. The proposed design permits many degrees of freedom by decoupling the performance parameters into several regions in the cavity. Thus a designer can optimize one performance parameters at a time without influence too much on the other performance parameters.*

## 1. Introduction

Micro ring resonator sensors have been demonstrated in many material platforms, such as SOI [1], SiN [2] and SiON [3]. Recently, a Yb<sup>3+</sup> doped Al<sub>2</sub>O<sub>3</sub> micro ring laser sensor has been demonstrated [4]. A lasing micro ring sensor has much narrower linewidth than its passive cavity, thus, in principle, can detect a much smaller resonant wavelength shift. Therefore, a lower detection limit is possible. However, since each physical parameter of the ring (such as waveguide width, thickness, ring radius, and gap size) is related to multiple performance parameters (such as sensitivity, free spectral range and laser threshold), it is difficult to optimize the performance of the laser cavity shown in Fig.1 (a). In order to have more control over the performance parameters, the proposed cavity, Fig.1 (b), decouples the performance parameters into several regions..

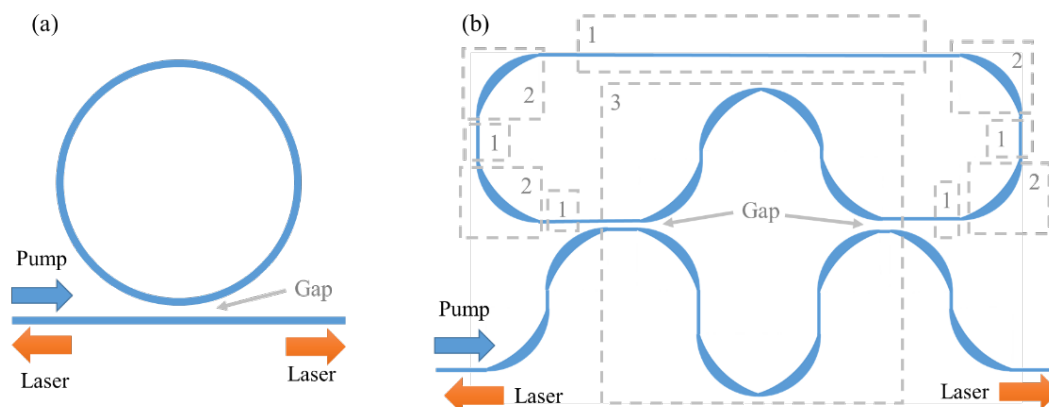


Fig.1. (a) Commonly used micro ring laser cavity. (b) Proposed micro ring laser cavity. The waveguide width and thickness of regions 1 (indicated with dashed gray boxes) mainly influence the sensitivity. The length of regions 1 is mainly used to tune the free spectral range. The regions 2 are adiabatic bends, which are designed to have negligible bend loss and straight to bend coupling loss. Region 3 is a Mach-Zehnder interferometer based Wavelength Division Multiplexing (WDM) coupler, which is used to tune the coupling strength of pumping and lasing wavelength.

## 2. Laser sensor cavity design

In the following section, the design methodology is described in detail with examples of designing sensitivity, bend loss, and spectral performance. All the examples are simulated for a Yb<sup>3+</sup> doped Al<sub>2</sub>O<sub>3</sub> channel waveguide with SiO<sub>2</sub> bottom cladding and H<sub>2</sub>O top cladding. Nevertheless, the design methodology is, in principle, applicable in other material platforms and waveguide geometries.

## 2.1 Sensitivity

In this example, the sensor should be sensitive to the bulk refractive index changes in H<sub>2</sub>O. This requires that the fraction,  $\eta$ , of the mode power in H<sub>2</sub>O is as high as possible. Waveguides with different width and height have been simulated and their fundamental TE modes are shown in Fig.2. (The micro ring laser typically lases in TE mode due to less bend losses in comparison with TM mode. Thus the simulations are focused on TE polarization.) The results indicate that a smaller core size is able to push the evanescent field further into the H<sub>2</sub>O cladding thus obtaining higher sensitivity. The minimal core width is typically limited by the lithography, which is about 1  $\mu\text{m}$  in our case. For a given core width, the minimal core height is limited by the bend loss described in the next section.

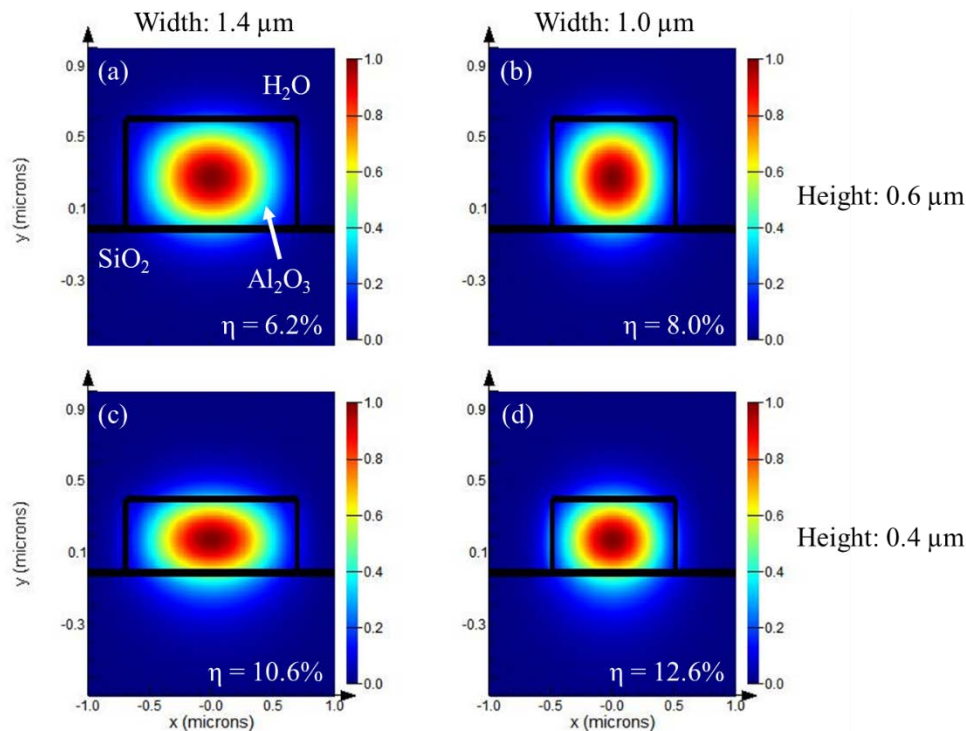


Fig.2. Mode calculations for waveguides with different core size. The fraction of the power in H<sub>2</sub>O is indicated with  $\eta$ . (a) Height 0.6  $\mu\text{m}$ , width 1.4  $\mu\text{m}$ . (b) Height 0.6  $\mu\text{m}$ , width 1.0  $\mu\text{m}$ . (c) Height 0.4  $\mu\text{m}$ , width 1.4  $\mu\text{m}$ . (d) Height 0.4  $\mu\text{m}$ , width 1.0  $\mu\text{m}$ .

## 2.2 Bend loss

The bend loss of a waveguide with 0.4  $\mu\text{m}$  height and 1.0  $\mu\text{m}$  width is simulated and shown in Fig.3 (a). The result shows a significant increase in bend loss as the bend radius decrease. In order to have a low threshold laser, the bend loss should be as small as possible. In our example, we set a target of  $\sim 0.1$  dB/cm which is much smaller than our typical propagation loss of  $< 0.5$  dB/cm. This target corresponding to a large bend radius of 230  $\mu\text{m}$ . One way to decrease the bend radius and keep the bend loss small is to increase the waveguide width as shown in Fig.3 (b). For a bend loss of 0.1 dB/cm, the bend radius can be as small as 75  $\mu\text{m}$ , with a waveguide width of 2.5  $\mu\text{m}$ .

Adiabatic bend described in Roeloffzen's paper [5] is a perfect component to connect the high sensitivity straight waveguide regions, as shown with the regions 2 in Fig.1 (b). Adiabatic bend is a bend that starts with a very large bend radius gradually reducing its bend radius to a minimal value and increasing it again as shown in Fig.4. As the bend

radius decreases, the waveguide width increases gradually to ensure a negligible bend loss at any point along the bend. A negligible straight-to-bend coupling loss also by having the very large bend radius at the beginning of the bend.

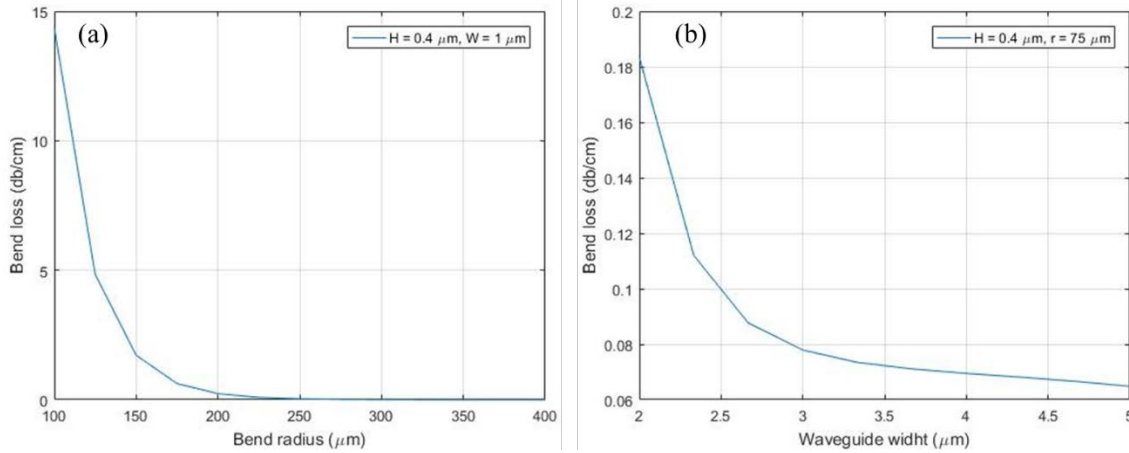


Fig.3. Bend loss simulation. (a) Bend loss at different bend radius for a waveguide with 0.4  $\mu\text{m}$  height and 1  $\mu\text{m}$  width. (b) Bend loss at different waveguide width for a bend radius of 75  $\mu\text{m}$  and 0.4  $\mu\text{m}$  height.

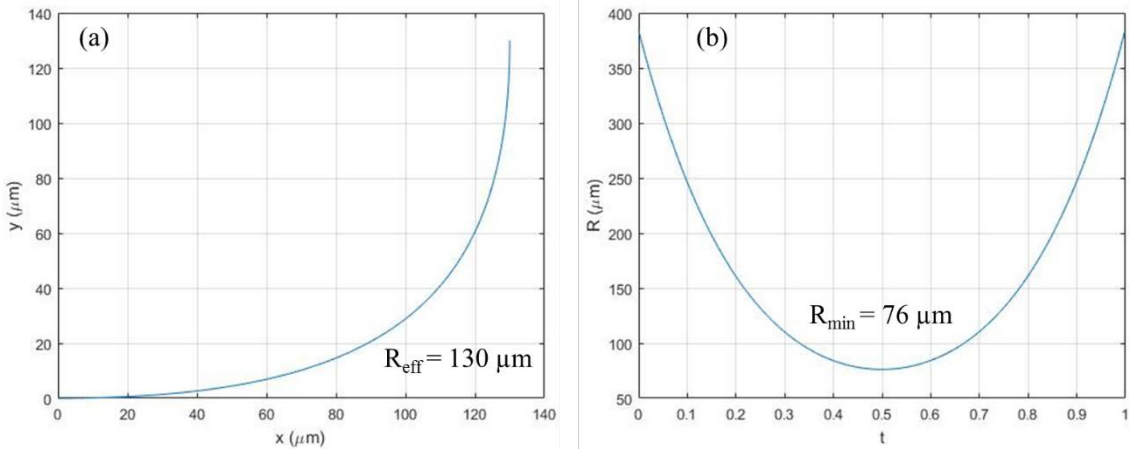


Fig.4. (a) Center path of an adiabatic bend defined by a third-order Bezier curve. The size of this bend is close to a normal bend with a radius of 130  $\mu\text{m}$ . (b) The radius of curvature,  $R$ , of the bend shown in (a), where the  $t$  is a parameter indicates the position along the bend.

### 2.3 Spectral performance

In a commonly used simple ring laser cavity, only a small fraction of pump power is coupled into the ring cavity. This leads to high pump power requirement. In order to increase the pump coupling efficiency, one can use a smaller gap or a larger ring. However, this leads to higher coupling loss at the lasing wavelength, thus a lower Q factor and higher lasing threshold.

In order to achieve high pump coupling efficiency, a WDM is proposed, as shown with the region 3 in Fig.1 (b). In this example, the WDM is based on a Mach-Zehnder interferometer design. It consists of two directional couplers (DCs) with lengths of  $L_{DC1}$  and  $L_{DC2}$ , respectively. There is a phase section in between the two DCs, which has a physical length difference of  $dL$  between the two arms. The gap size of each DC is chosen based on the fabrication reliability, which is 0.9  $\mu\text{m}$  in our case. One can then design the pump coupling efficiency with the total length of  $L_{DC1}$  and  $L_{DC2}$ . The lasing wavelength is chosen by the  $dL$  such that the pump wavelength has a phase delay of  $N*2\pi$ , where  $N$  is an integer, and the lasing wavelength has a phase delay of  $N*2\pi-\pi$ . The lasing

wavelength power coupling can be designed with the length difference of  $L_{DC1}$  and  $L_{DC2}$ . A WDM example has been simulated and shown in Fig.5. In this example, the pump wavelength is 976 nm which have 82% coupling efficiency into the laser cavity. The lasing wavelength is 1028 nm which has 2.2% coupling efficiency. The laser threshold and slope efficiency depend on the lasing wavelength coupling efficiency, which can be designed by the length difference of  $L_{DC1}$  and  $L_{DC2}$ .

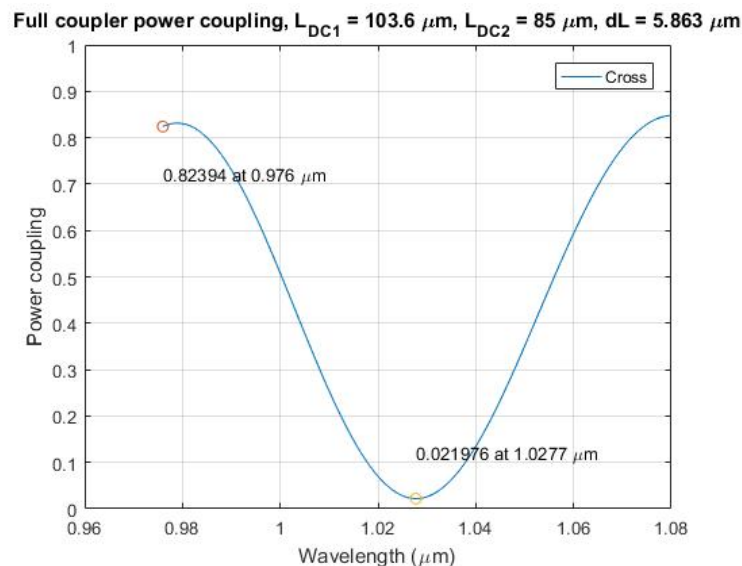


Fig.5. A simulated WDM spectrum.

### 3. Conclusions

The proposed cavity design enables a designer to tune or optimize one set of performance parameter at a given region without influencing too much on other performance parameters. This leads to more design freedom and less compromise compared with a commonly used simple ring cavity.

### Acknowledgments

This project has received funding from the European Union's Horizon 2020 research and innovation program, GLAM, under grant agreement No 634928.

### References

- [1] W. Bogaerts, P. De Heyn, T. Van Vaerenbergh, K. De Vos, S. K. Selvaraja, T. Claes, P. Dumon, P. Bienstman, D. Van Thourhout, and R. Baets, "Silicon microring resonators," *Laser Photonics Rev* **6**, 47-73, 2012.
- [2] K. Worhoff, R. G. Heideman, A. Leinse, and M. Hoekman, "TriPleX: a versatile dielectric photonic platform," *Adv Opt Technol* **4**, 189-207, 2015.
- [3] A. Samusenko, D. Gandolfi, G. Pucker, T. Chalyan, R. Guider, M. Ghulinyan, and L. Pavesi, "A SiON Microring Resonator-Based Platform for Biosensing at 850 nm," *J Lightwave Technol* **34**, 969-977, 2016.
- [4] M. de Goede, L. Chang, M. Dijkstra, R. Obregón, J. Ramón-Azcón, E. Martínez, L. Padilla, J. Adan, F. Mitjans, and S. M. García-Blanco, "Al<sub>2</sub>O<sub>3</sub> Microresonators for Passive and Active Sensing Applications," in *Advanced Photonics 2018 (BGPP, IPR, NP, NOMA, Sensors, Networks, SPPCom, SOF)*, OSA Technical Digest (online) (Optical Society of America, 2018), SeTu4E.1.
- [5] C.G.H. Roeloffzen, R.M. de Ridder, and A. Driessen, "Low-loss adiabatic bend using minimised chip area," in *Proceedings 2000 IEEE/LEOS Symposium Benelux Chapter*, X.J.M. Leijtens and J.H. Besten, Editors. 2000, Delft University of Technology: Delft. p. 175-178.